

# Identification of the Benzyloxyphenyl Pharmacophore: A Structural Unit That Promotes Sodium Channel Slow Inactivation

Amber M. King,<sup>†,∇</sup> Xiao-Fang Yang,<sup>§,#,∇</sup> Yuying Wang,<sup>§,∇</sup> Erik T. Dustrude,<sup>#</sup> Cindy Barbosa,<sup>§</sup> Michael R. Due,<sup>⊥</sup> Andrew D. Piekarczyk,<sup>§</sup> Sarah M. Wilson,<sup>#</sup> Fletcher A. White,<sup>§,⊥,#</sup> Christophe Salomé,<sup>†</sup> Theodore R. Cummins,<sup>§,#</sup> Rajesh Khanna,<sup>\*,§,||,#</sup> and Harold Kohn<sup>\*,†,‡</sup>

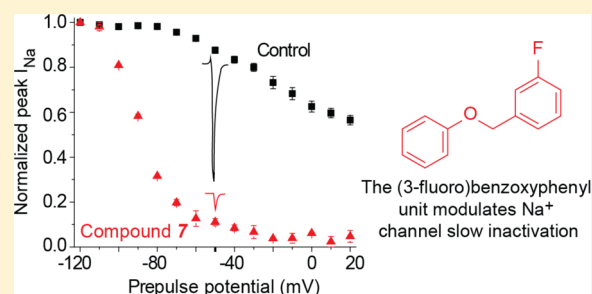
<sup>†</sup>Division of Chemical Biology and Medicinal Chemistry, UNC Eshelman School of Pharmacy, and <sup>‡</sup>Department of Chemistry, University of North Carolina, Chapel Hill, North Carolina 27599, United States

<sup>§</sup>Departments of Pharmacology & Toxicology, <sup>||</sup>Biochemistry & Molecular Biology, and <sup>⊥</sup>Anesthesia and <sup>#</sup>Program in Medical Neuroscience, Paul and Carole Stark Neurosciences Research Institute, Indiana University School of Medicine, Indianapolis, Indiana 46202, United States

**ABSTRACT:** Four compounds that contained the *N*-benzyl 2-amino-3-methoxypropionamide unit were evaluated for their ability to modulate Na<sup>+</sup> currents in catecholamine A differentiated CAD neuronal cells. The compounds differed by the absence or presence of either a terminal *N*-acetyl group or a (3-fluoro)benzyloxy moiety positioned at the 4'-benzylamide site. Analysis of whole-cell patch-clamp electrophysiology data showed that the incorporation of the (3-fluoro)benzyloxy unit, to give the (3-fluoro)benzyloxyphenyl pharmacophore, dramatically enhanced the magnitude of Na<sup>+</sup> channel slow inactivation. In addition, *N*-acetylation markedly increased the stereoselectivity for Na<sup>+</sup> channel slow inactivation.

Furthermore, we observed that Na<sup>+</sup> channel frequency (use)-dependent block was maintained upon inclusion of this pharmacophore. Confirmation of the importance of the (3-fluoro)benzyloxyphenyl pharmacophore was shown by examining compounds where the *N*-benzyl 2-amino-3-methoxypropionamide unit was replaced by a *N*-benzyl 2-amino-3-methylpropionamide moiety, as well as examining a series of compounds that did not contain an amino acid group but retained the pharmacophore unit. Collectively, the data indicated that the (3-fluoro)benzyloxyphenyl unit is a novel pharmacophore for the modulation of Na<sup>+</sup> currents.

**KEYWORDS:** Benzyloxyphenyl pharmacophore, voltage-gated sodium channels, slow inactivation, anticonvulsant activity, hyperexcitable neurons, epilepsy



Epilepsy is a serious neurological disorder affecting up to 1% of the world's population.<sup>1</sup> It is a common misconception that epilepsy is a single disease; rather, epilepsy is a heterogeneous mixture of disorders characterized by reoccurring, unprovoked seizures that result from neuronal hyperexcitability and hypersynchronous neuronal firing.<sup>1,2</sup> Pharmacological management is the primary treatment option, but 30% of patients are pharmacoresistant and do not respond to at least two of the first-line antiepileptic drugs (AEDs),<sup>3</sup> and those who do respond often experience adverse side effects (e.g., drowsiness, dizziness, nausea).<sup>4</sup> Therefore, new AEDs with novel mechanisms of action are needed to improve the outlook of the pharmacological management of epilepsy.

We have reported on the anticonvulsant activities in the maximal electroshock seizure (MES) model<sup>5</sup> of four classes of compounds that contained an *N*-benzyl 2-amino-3-methoxypropionamide (**A**) structural unit, where the R and R' substituents and the C(2) stereochemistry were varied.<sup>6–12</sup> Included in this set was the parent compound **1** (R, R' = H),<sup>7,8,11</sup> the *N*-acetylated derivative **2** (R = CH<sub>3</sub>C(O), R' = H),<sup>6</sup> the 4'-benzyl modified compound **3** (R = H, R' =

OCH<sub>2</sub>Ph(*m*-F)),<sup>12</sup> and the disubstituted analogue **4** (R = CH<sub>3</sub>C(O), R' = OCH<sub>2</sub>Ph(*m*-F)).<sup>10</sup> We observed that **2–4** exhibited potent anticonvulsant activities,<sup>6,10,12</sup> and that for compounds **1–4**, increased anticonvulsant activity was associated with the *D*-amino configuration ((*R*)-stereoisomer).<sup>6,8,10–12</sup> The anticonvulsant activities of (*R*)-**2**, (*R*)-**3**, and (*R*)-**4** rivaled the anticonvulsant activities of clinically used AEDs.<sup>13</sup> One of these compounds, (*R*)-*N*-benzyl 2-acetamido-3-methoxypropionamide<sup>6</sup> (lacosamide, (*R*)-**2**), is a first-in-class AED marketed in 34 countries, including the United States.<sup>14</sup> Studies have shown that (*R*)-**2** preferentially transitioned voltage-gated Na<sup>+</sup> channels (VGSCs) to the slow inactivation state without affecting fast inactivation.<sup>15–17</sup> Na<sup>+</sup> channel slow inactivation promotion is a powerful mechanism to control the hyperexcitable neuron in the epileptic patient, where neurons are either rapidly firing or in a sustained, depolarized state.

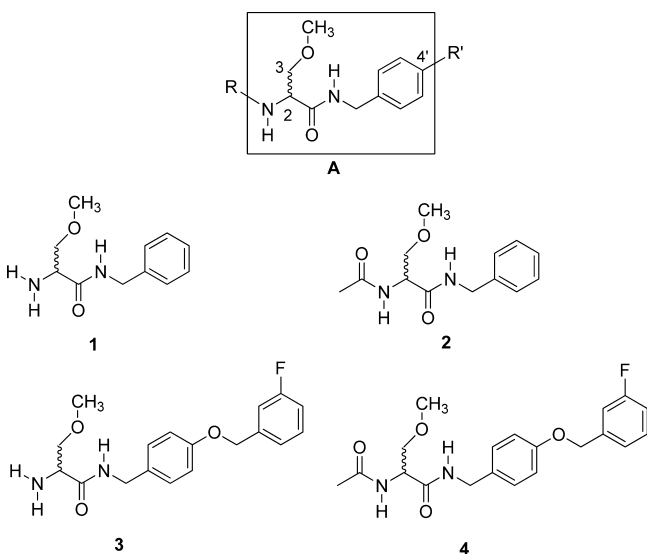
Received: August 16, 2012

Accepted: September 19, 2012

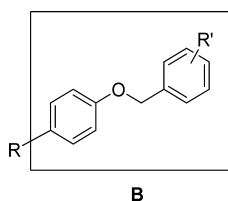
Published: September 19, 2012



Neuropathic pain, like epilepsy, results from neuronal hyperexcitability.<sup>18</sup> Compound (*R*)-**2** has been evaluated in several neuropathic pain animal models with success,<sup>19</sup> a finding consistent with pharmacological and clinical studies that document the similarities in the pathophysiological phenomena observed in epilepsy and neuropathic pain models.<sup>20,21</sup>



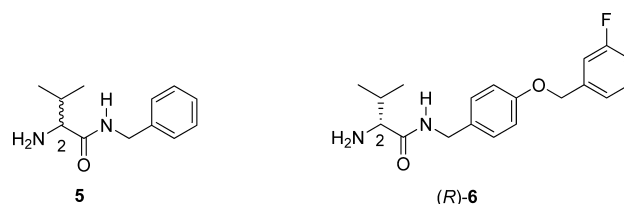
In this investigation, we compare the Na<sup>+</sup> channel properties of **1** and **3** with those reported for **2**<sup>15–17</sup> and **4**.<sup>10,22</sup> We show that (*R*)-**1**, like (*R*)-**2**, promotes Na<sup>+</sup> channel slow inactivation, and that *N*-acetylation of the terminal amine in (*R*)-**1** markedly increases the stereoselectivity of this process. We further document that 4'-aryl extension of (*R*)-**1** and (*R*)-**2** to give (*R*)-**3** and (*R*)-**4**, respectively, dramatically enhance Na<sup>+</sup> channel slow inactivation. Analysis of the data identifies the substituted benzyloxyphenyl (**B**) unit as a pharmacophore that can transition Na<sup>+</sup> channels to the slow inactivation conformation. We confirm these findings by testing the Na<sup>+</sup> channel properties of additional compounds.



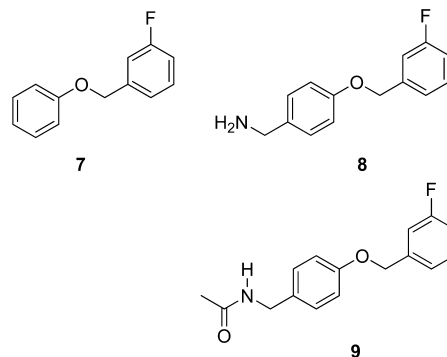
## RESULTS AND DISCUSSION

**Choice of Compounds and Synthesis.** Our initial study on the effect of chemical structure on Na<sup>+</sup> channel modulation was restricted to compounds **1–4** that contained the *N*-benzyl 2-amino-3-methoxypropionamide (**A**) moiety. Our previous studies guided our compound selection.<sup>6,10–12</sup> Compounds (*R*)-**2–(R)**-**4** exhibited excellent anticonvulsant activity in the MES test (MES ED<sub>50</sub> (mg/kg, mice (ip)): (*R*)-**2**, 4.5; (*R*)-**3**, 15; (*R*)-**4**, 13)) that exceeded the anticonvulsant activity of phenobarbital (MES ED<sub>50</sub> = 22 mg/kg) (Table 1). Compounds **1** and **3** did not possess an *N*-acetyl moiety, while **2** and **4** did. Compounds **3** and **4** are 4'-aryl extended analogs of **1** and **2**, respectively. For compounds **1**, **2**, and **4**, we examined both the (*R*)- and (*S*)-stereoisomers because anticonvulsant activity was associated with the (*R*)-configuration.<sup>6,10,11</sup> The Na<sup>+</sup> channel

properties observed for **1–4** prompted us to investigate amino acid derivatives that did not contain the 2-amino-3-methoxypropionic acid unit, but still possessed either the *N*-benzyl amide or the *N*-4'-(3-fluoro)benzyloxybenzyl amide group seen in either **1** and **2**, or **3** and **4**, respectively. Thus, we examined (*R*)-**5**,<sup>11</sup> (*S*)-**5**,<sup>11</sup> and (*R*)-**6**,<sup>12</sup> where we replaced the 2-amino-3-methoxypropionic acid unit with a 2-amino-3-methylpropionic acid group. We chose (*R*)-**5** and (*R*)-**6** because of their excellent anticonvulsant activities in the MES test.<sup>11,12</sup> Compound (*R*)-**5** was one the most potent C(2)-hydrocarbon derivatives tested.<sup>11</sup> The MES ED<sub>50</sub> values in mice (ip) for (*R*)-**5** and (*R*)-**6** were 15 and 12 mg/kg, respectively (Table 1). Notably, (*R*)-**6** contained both a 2-amino-3-methylpropionic acid group and a (3-fluoro)benzyloxyphenyl unit.



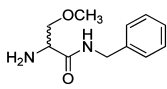
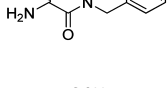
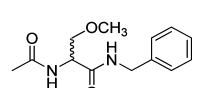
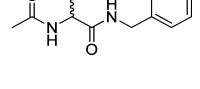
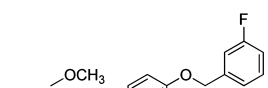
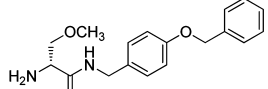
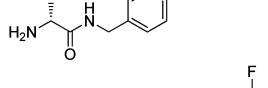
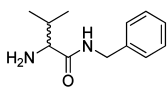
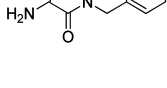
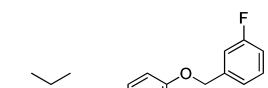
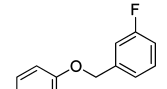
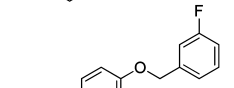
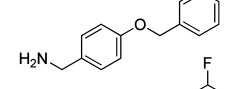
Next, we tested compounds **7–9**. All three compounds possessed a 4'-(3-fluoro)benzyloxyphenyl unit, but did not contain an amino acid group. The synthesis of **1–6**, **8**, and **9** were previously reported, and compound **7** is commercially available.



### Modulation of Na<sup>+</sup> Channel Slow Inactivation by Compounds **1–4**.

Using the whole-cell patch-clamp configuration, we examined the effects of **1–4** on VGSCs in the catecholamine A differentiated (CAD) neuronal cell line. We have previously shown that CAD cells were surrogates of neuronal cell lines and express endogenous tetrodotoxin-sensitive Na<sup>+</sup> currents with rapid activation and inactivation upon membrane depolarization, and are likely composed of Na<sub>v</sub>1.7, Na<sub>v</sub>1.1, and Na<sub>v</sub>1.3 channels.<sup>23</sup> Na<sub>v</sub>1.7 mRNA is expressed at 15- and 30-fold higher levels compared with mRNAs of Na<sub>v</sub>1.1 and Na<sub>v</sub>1.3, respectively.<sup>23</sup> Consistent with this level of expression, we confirmed that the majority of the Na<sub>v</sub> current was carried via Na<sub>v</sub>1.7, as >55% of the current was blocked by Na<sub>v</sub>1.7-selective protox II (10 nM, see Figure 8A, B). We previously found that the Na<sup>+</sup> channel properties of (*R*)-**2** in CAD cells<sup>23</sup> were similar to those reported in cultured rat cortical neurons and mouse N1E-115 neuroblastoma cells.<sup>15</sup> Accordingly, we initially used readily accessible CAD cells to evaluate the effect of structure on neuronal function, recognizing in advance that CAD cells do not express the same complement of Na<sup>+</sup> channels expressed in CNS neurons. In additional pilot studies, we verified that (*R*)-**1–(R)**-**4**, as well

Table 1. Anticonvulsant and Electrophysiology Data for Test Compounds

Cmpd No.	Whole Animal Behavioral Studies				Maximal Slow Inactivation IC <sub>50</sub> <sup>f</sup> (at +20 mV; μM)
	Mice (ip) <sup>a</sup>		Rat (po) <sup>b</sup>		
	MES, <sup>c</sup> ED <sub>50</sub>	Tox, <sup>d</sup> TD <sub>50</sub>	MES, <sup>c</sup> ED <sub>50</sub>	Tox, <sup>e</sup> TD <sub>50</sub>	
 (R)-1 <sup>g</sup>	34	>120	ND <sup>h</sup>	ND <sup>h</sup>	100
 (S)-1 <sup>g</sup>	64	63	ND <sup>h</sup>	ND <sup>h</sup>	81
 (R)-2 <sup>i</sup>	4.5 [0.5] (3.7–5.5)	27 [0.25] (26–28)	3.9 [2.0] (2.9–6.2)	>500	120
 (S)-2 <sup>i</sup>	>100, <300	>300	>30	>30	>2500
 (R)-3 <sup>j</sup>	15 [0.5] (13–17)	58 [0.25] (53–62)	13 [0.5] (10–18)	>500	70
 (R)-4 <sup>k</sup>	13 [0.25] (11–16)	26 [0.5] (21–34)	14 [0.5] (6.1–27)	>500 [0.5]	0.30
 (S)-4 <sup>k</sup>	>300	>300	ND <sup>h</sup>	ND <sup>h</sup>	330
 (R)-5 <sup>g</sup>	15 [0.25] (13–18)	70 [0.25] (63–80)	11 [0.25] (9.1–13)	>500	940
 (S)-5 <sup>g</sup>	>300 [0.5]	>300 [0.5]	ND <sup>h</sup>	ND <sup>h</sup>	>1000
 (R)-6 <sup>j</sup>	12	ND <sup>h</sup>	13 [0.5] (10–18)	>500	0.60
 7	ND <sup>h</sup>	ND <sup>h</sup>	ND <sup>h</sup>	ND <sup>h</sup>	2.3
 8 <sup>k</sup>	ND <sup>h</sup>	ND <sup>h</sup>	ND <sup>h</sup>	ND <sup>h</sup>	10
 9	ND <sup>h</sup>	ND <sup>h</sup>	ND <sup>h</sup>	ND <sup>h</sup>	12
phenytoin <sup>l</sup>	9.5 [2.0] (8.1–10)	27 [0.25] (26–28)	30 [4.0] (22–39)	>3000	NS <sup>m</sup>
phenobarbital <sup>l</sup>	22 [1.0] (15–23)	66 [0.5] (63–73)	9.1 [5.0] (7.6–12)	61 [0.5] (44–96)	NS <sup>m</sup>
valproate <sup>l</sup>	270 [0.5] (250–340)	430 [0.25] (370–450)	490 [0.5] (350–730)	280 [0.5] (190–350)	NS <sup>m</sup>

<sup>a</sup>The compounds were administered intraperitoneally to adult male albino CF-1 mice or NMRI mice. ED<sub>50</sub> and TD<sub>50</sub> values are in mg/kg. A dose–response curve was generated for all compounds that displayed sufficient activity and the dose–effect data for these compounds was obtained at the “time of peak effect” (indicated in hours in the brackets). Numbers in parentheses are 95% confidence intervals. <sup>b</sup>The compounds were administered orally to adult male albino Sprague–Dawley rats. ED<sub>50</sub> and TD<sub>50</sub> values are in mg/kg. <sup>c</sup>MES = maximal electroshock seizure test. <sup>d</sup>Tox = neurological toxicity. TD<sub>50</sub> value determined from the rotorod test. <sup>e</sup>Tox = behavioral toxicity. <sup>f</sup>IC<sub>50</sub>, Concentration at which half of the Na<sup>+</sup> channels have transitioned to a slow inactivated state. <sup>g</sup>Reference 11. <sup>h</sup>ND = not determined. <sup>i</sup>Reference 6. <sup>j</sup>Reference 12. <sup>k</sup>Reference 10. <sup>l</sup>Reference 13. <sup>m</sup>NS = not selective for slow inactivation.

as their enantiomers, were capable of inhibiting  $\text{Na}^+$  currents in CAD cells without affecting reversal potential (data not shown), half-maximal activation (see Figure 3), or slope parameters (data not shown).

To measure the effect of compounds 1–4 on  $\text{Na}^+$  channel slow inactivation, a cardinal feature of (R)-2<sup>23</sup> and (R)-4,<sup>22</sup> we held CAD cells at  $-80$  mV and conditioned them to potentials ranging from  $-120$  mV to  $+20$  mV (in 10 mV increments) for 5 s.<sup>22,23</sup> Then, fast-inactivated channels were allowed to recover for 150 ms at a hyperpolarized pulse to  $-120$  mV, and the fraction of channels available was tested by a single depolarizing pulse to 0 mV for 15 ms. This brief hyperpolarization allowed the channels to recover from fast inactivation while limiting recovery from slow inactivation. Using this protocol (Figure 1A), we generated a series of compound response curves showing the normalized peak ( $I_{\text{Na}}$ ) versus prepulse potential (mV) at a given compound concentration. The maximal  $\text{IC}_{50}$  values (in  $\mu\text{M}$ ) at  $+20$  mV for each compound listed in Table 1 were determined from the response curves generated from a series of compound concentrations. The  $+20$  mV potential was chosen because maximal slow inactivation is achieved at this potential, and derivation of maximal  $\text{IC}_{50}$  values is likely to unmask even subtle effects of chemical modification to the test compounds on slow inactivation. To illustrate the effects of compounds on slow inactivation, we have also presented the data at  $-50$  mV. The potential of  $-50$  mV was chosen for three reasons: (1) a large fraction of the channels undergo steady-state inactivation, which involves contributions from slow and fast inactivation pathways,<sup>24,25</sup> where  $-50$  mV is within the steep voltage-dependence range for each, (2) it is near the resting membrane potential and approaches the action potential firing threshold for central nervous system neurons,<sup>26</sup> where slow inactivation appears to be physiologically relevant during sustained subthreshold depolarizations,<sup>27</sup> and (3) changes in the  $\text{Na}^+$  channel availability near  $-50$  mV can impact the overlap of  $\text{Na}^+$  current activation and inactivation under steady-state conditions.<sup>25,28</sup> Representative traces illustrating the extent of slow inactivation observed at  $-50$  mV compared to the prepulse at  $-10$  mV in the absence or presence of (R)-1, (S)-1, and (R)-3 are shown in Figure 1B, with complete slow inactivation curves (normalized peak versus prepulse potential) shown in Figure 1C. A lesser concentration of (R)-3 ( $100 \mu\text{M}$  versus  $500 \mu\text{M}$  for (R)-1 and (R)-2), in which the (3-fluoro)benzyloxy substituent has been appended to the 4'-benzyl site in (R)-1 to provide the (3-fluoro)benzyloxyphenyl pharmacophore, is shown to highlight the superior slow inactivation-promoting capability of (R)-3 compared with (R)-1 and (R)-2 (Figure 1C, D). Importantly, (R)-4, which has both a 4'-(3-fluoro)benzyloxy substituent and a *N*-acetyl moiety, demonstrated the highest extent of slow inactivation, as even  $30 \mu\text{M}$  of (R)-4 was better at transitioning  $\text{Na}^+$  channels into the slow inactivated state compared with  $100 \mu\text{M}$  or more of (R)-1, (S)-1, and (R)-3 (Figure 1D).

*N*-Acetylation of *N*-benzyl 2-amino-3-methoxypropionamide (1) to provide *N*-benzyl 2-acetamido-3-methoxypropionamide (2) markedly increased the stereoselectivity for  $\text{Na}^+$  channel slow inactivation (maximal slow inactivation  $\text{IC}_{50}$  at  $+20$  mV): (S)-1/(R)-1 = 0.81; (S)-2/(R)-2 = > 21 (Figure 2). We found a more dramatic change in the stereoselectivity in  $\text{Na}^+$  channel slow inactivation modulation for 4, which contained both the

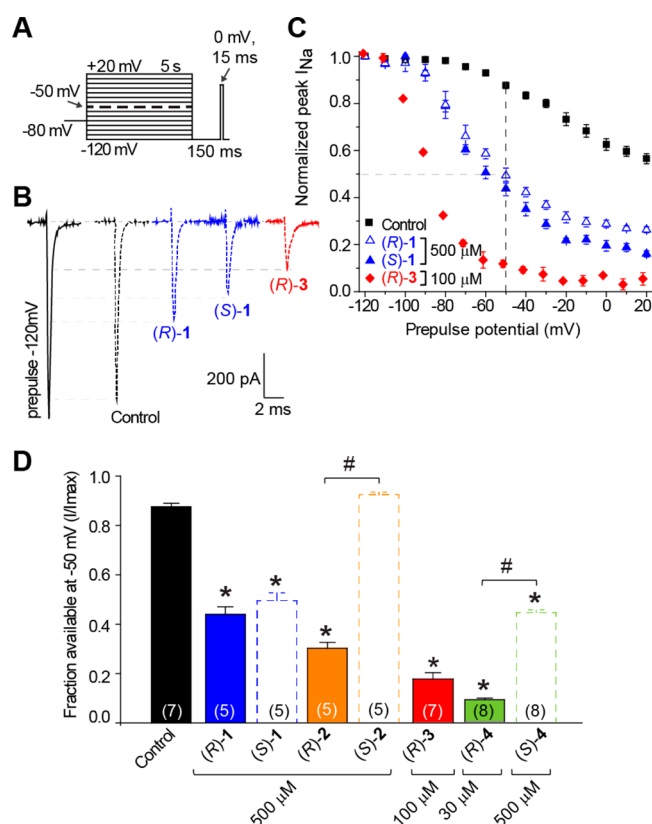


**Figure 1.** Effect of *N*-acetylation and 4'-aryl extension in *N*-benzyl 2-amino-3-methoxypropionamide derivatives on slow inactivated  $\text{Na}^+$  currents in CAD cells. (A) Voltage protocol for slow inactivation: currents were evoked by 5 s prepulses between  $-120$  and  $+20$  mV, and then fast inactivated channels were allowed to recover for 150 ms at a hyperpolarized pulse to  $-120$  mV. The fraction of channels available at 0 mV was analyzed. (B) Representative current traces from CAD cells in the absence (control, 0.1% DMSO; solid trace) or presence of  $500 \mu\text{M}$  of (R)-1 and (S)-1, or  $100 \mu\text{M}$  of (R)-3 (dashed traces). As a comparator of the extent of slow inactivation, the control trace at  $-120$  mV (prepulse) is also shown (solid trace). (C) Summary of steady-state, slow inactivation curves for CAD cells treated with DMSO (control),  $500 \mu\text{M}$  (R)-1 and (S)-1 or  $100 \mu\text{M}$  (R)-3. Drug-induced slow inactivation was almost equivalent in CAD cells treated with (R)-1 and (S)-1, but was more prominent with (R)-3. Some error bars are smaller than the symbols. In this and subsequent figures, data are presented as means  $\pm$  SEM. (D) Summary of the fraction of current available at  $-50$  mV for CAD cells in the absence or presence of (R)- or (S)-enantiomers of the indicated compounds. Asterisks indicate statistically significant differences in fraction of current available between predrug and (R)- and (S)-compounds ( $p < 0.05$ , one-way ANOVA with Dunnett's posthoc test). Hash mark indicates a statistically significant difference in fraction of current available between (R)- and (S)-enantiomers. Numbers in parentheses are the number of cells patched per condition. The half-maximal values for slow inactivation for these compounds are shown in Table 1.

4'-(3-fluoro)benzyloxyphenyl substituent and the *N*-acetyl moiety. The maximal slow inactivation  $\text{IC}_{50}$  ratio at  $+20$  mV for (S)-4/(R)-4 was 1100, indicating that the combination of the *N*-acetyl and the (3-fluoro)benzyloxyphenyl moieties increased both the potency and the stereoselectivity for  $\text{Na}^+$  channel function. Together these results demonstrated that

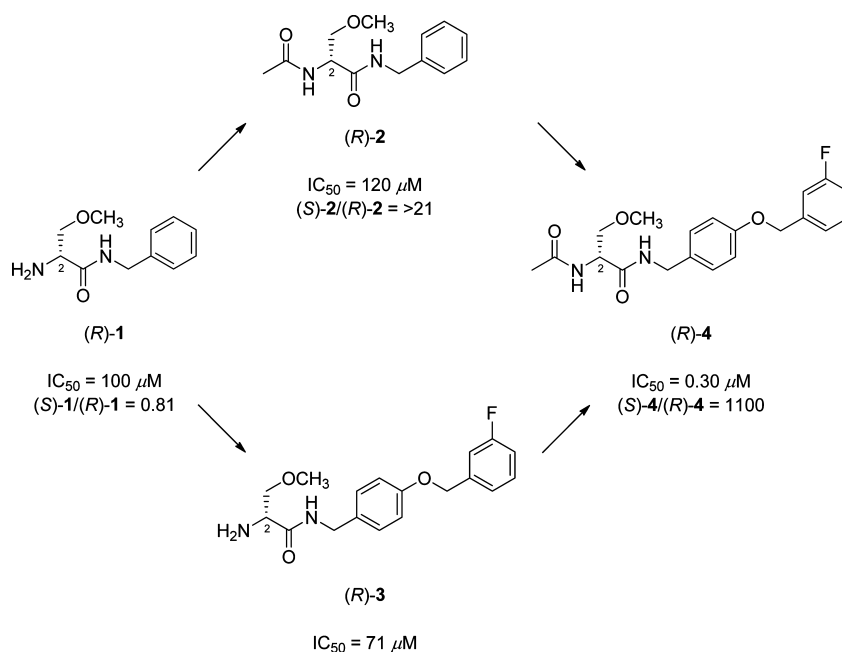


**Figure 2.** Effect of *N*-acetylation and inclusion of a 4'-extended aryl group ((3-fluoro)benzyloxy) on (*R*)-1 for Na<sup>+</sup> channel slow inactivation potency and stereoselectivity for function. Changes in the Na<sup>+</sup> channel maximal slow inactivation  $IC_{50}$  value (+20 mV) and stereoselectivity as a function of structure.

(*R*)-4 is an effective ligand for the receptor(s) responsible for mediating Na<sup>+</sup> channel slow inactivation.

**Modulation of Steady-State Activation, Fast Inactivation, and Frequency Dependent Block of Na<sup>+</sup> Channels by (*R*)-1–(*R*)-4.** While promotion of slow inactivation is a hallmark of (*R*)-2, we investigated if changing (*R*)-2 by either deleting the *N*-acetyl moiety or adding the 4'-(3-fluoro)benzyloxy substituent affected other biophysical properties, namely, steady-state activation, fast inactivation, and frequency-dependent block. Changes in activation for the CAD cells treated with the test compounds were measured by whole-cell ionic conductances (in response to a voltage protocol shown in Figure 3A, inset left) by comparing their midpoints ( $V_{1/2}$ ) and slope factors ( $k$ ) in response to changes in command voltage. Representative Boltzmann fits for DMSO (control) and 30–500  $\mu M$  1–4 are shown in Figure 3. An analysis of  $V_{1/2}$  and  $k$  values derived from the Boltzmann fits showed that there were no changes in the steady-state activation properties of Na<sup>+</sup> currents between CAD cells treated with DMSO control or the highest concentrations of 1–4 (data not shown). These data indicate that the compounds do not affect the channel's transition from a closed to an open conformation.

In addition to affecting slow inactivation, stabilization of the fast-inactivated conformation that is rapidly generated upon channel firing is one possible way to control neuronal hyperexcitability. Most anticonvulsants whose activity is attributed, in part, to Na<sup>+</sup> channel inactivation stabilize the fast-inactivated conformation.<sup>29</sup> Accordingly, we tested whether 1–4 affected Na<sup>+</sup> channel fast inactivation using a protocol designed to induce a fast-inactivated state (voltage protocol shown in Figure 3B, inset right). Steady-state, fast inactivation curves of Na<sup>+</sup> currents from DMSO- and all 1–4-treated CAD cells were well fitted with a single Boltzmann function ( $R^2 > 0.9942$  for all conditions). The  $V_{1/2}$  value for inactivation for 0.1% DMSO-treated cells was  $-68.2 \pm 1.9$  mV ( $n = 8$ ), which was significantly different from that of (*R*)-4 (30  $\mu M$ )-treated

cells ( $-86.3 \pm 3.2$  mV;  $n = 8$ ;  $p < 0.05$ ; Student's *t* test; Figure 3B). Compared with the  $\sim 18.1$  mV shift in  $V_{1/2}$  of fast inactivation in the hyperpolarizing direction observed in the presence of (*R*)-4, the shifts caused by the other compounds were 15.8 mV, (*S*)-4 (500  $\mu M$ ;  $n = 6$ ); 0.8 mV, (*R*)-1 (500  $\mu M$ ;  $n = 7$ ); 0.9 mV, (*S*)-1 (500  $\mu M$ ;  $n = 7$ ); and 0.1 mV, (*R*)-3 (30  $\mu M$ ;  $n = 7$ ; Figure 3) ( $p < 0.05$  vs DMSO control; Student's *t* test). By comparison, we observed a 0.3 mV shift with (*R*)-2 (30  $\mu M$ ;  $n = 6$ ) and (*S*)-2 (500  $\mu M$ ;  $n = 6$ ), similar to the 0.7 mV shift 30 we had previously reported with (*R*)-2 (30  $\mu M$ ).<sup>22,23</sup>

Blockade of Na<sup>+</sup> currents in an activity- or frequency (use)-dependent manner is a useful property for AEDs because it favors decreased Na<sup>+</sup> channel activity during high-frequency (i.e., seizures) but not low-frequency firing.<sup>22,29</sup> Thus, we tested if (*R*)-1–(*R*)-4 could elicit frequency-dependent block (Figure 4). In pilot experiments, we determined that concentrations up to 100  $\mu M$  did not affect fast inactivation; therefore, a concentration of 30  $\mu M$  was used to compare the effects of (*R*)-1–(*R*)-4 on frequency-dependence. A train of 30 test pulses (20 ms to  $-10$  mV) was delivered from a holding potential of  $-80$  mV at 10 Hz.<sup>22</sup> The available current in the control and in the presence of the test compounds was calculated by dividing the peak current at any given pulse ( $\text{pulse}_N$ ) by the peak current in response to the initial pulse ( $\text{pulse}_1$ ). We observed appreciable frequency-dependent block for all compounds except (*R*)-2, with (*R*)-1, (*R*)-3, and (*R*)-4 being equally effective. The block developed quickly with (*R*)-1 and (*R*)-3 (between pulse 2 and 4) and plateaued by the sixth pulse, whereas the frequency-dependent block of (*R*)-4 was more gradual, reaching a plateau approximately after the 26th pulse. To show that (*R*)-4-induced use-dependence was reversible, we used conditions to washout any unbound (*R*)-4 and then tested for the extent of use-dependence. Incubation of CAD cell with 30  $\mu M$  of (*R*)-4 followed by a series of three washes with fresh extracellular bath solution over a 10 min

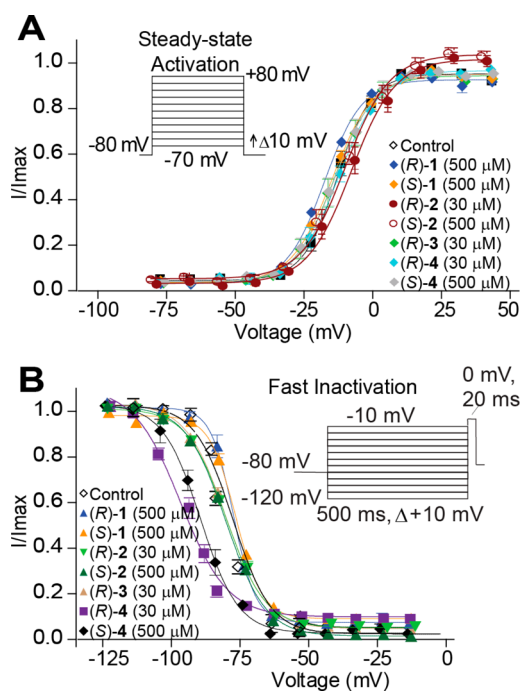


**Figure 3.** Effect of *N*-acetylation and 4'-aryl extension in *N*-benzyl 2-amino-3-methoxypropionamide on activation and fast inactivation properties of Na<sup>+</sup> currents in CAD cells. Values for  $V_{1/2}$ , the voltage of half-maximal activation (A) or inactivation (B), were derived from Boltzmann distribution fits to the individual recordings and averaged to determine the mean ( $\pm$ SEM) voltage dependence of activation (A) or inactivation (B), respectively. The voltage protocol used to evoke current responses is shown adjacent to the curves. Representative Boltzmann fits for 0.1–1% DMSO (control) and various concentrations of the compounds are shown. The  $V_{1/2}$  and  $k$  (slope; not shown) of activation (A) were not different among any of the compounds tested ( $p > 0.05$ , one-way ANOVA). Compound (R)-4 (30  $\mu$ M) induced a  $\sim$ 18.1 mV hyperpolarizing shift in the  $V_{1/2}$  of fast inactivation (B), while its enantiomer (S)-4 (500  $\mu$ M) caused a 15.8 mV shift. For all experiments, data are from 3–9 cells per condition.

period led to a complete elimination of use-dependence (Figure 4B–D). Collectively, these data show that the (3-fluoro)-benzyloxyphenyl substituent within (R)-3 and (R)-4 may be an effective pharmacophore for inducing reversible frequency-dependent block of Na<sup>+</sup> currents, but its presence is not obligatory.

#### Modulation of Neuronal Excitability of Dissociated Medium Diameter DRG Neurons by Compounds 1–4.

To examine the possibility that 1–4 affect the neuronal excitability of dissociated dorsal root ganglion (DRG) neurons, we tested medium DRG neuronal excitability before and after the addition of compounds. The excitability was measured by injecting current pulses (nA) into the soma of medium diameter DRG neurons every 30 s in order to elicit 8–12 action potentials under control conditions prior to the addition of 100  $\mu$ M of 1–4 into the recording bath. Representative recordings (Figure 5A) and grouped data (Figure 5B) show that the excitability (i.e., number of action potentials) of medium diameter DRG neurons was decreased  $>50\%$  by (R)-2, (R)-3, (R)-4, and to a small extent ( $\sim 15\%$ ) by (S)-1, but not by (R)-1, (S)-2, and (S)-4. These results suggest that the inclusion of both the 4'-(3-fluoro)benzyloxyphenyl substituent and the *N*-acetyl moiety in (R)-4 increased the potency and the stereoselectivity for inhibition of excitability in DRG neurons.

The relative activities of 1–4 in DRG neurons paralleled the CAD cell slow inactivation  $IC_{50}$  values for these compounds (Table 1), a finding consistent with the presence on Na<sub>v</sub>1.7 channels in both of these cells.<sup>23,30,31</sup>

**Structural Confirmation of the Benzyloxyphenyl Unit B in Promoting Na<sup>+</sup> Channel Slow Inactivation: Determination of the Na<sup>+</sup> Channel Properties of (R)-5, (S)-5, (R)-6, and 7–9.** The marked increase in the degree of Na<sup>+</sup> channel slow inactivation upon the appendage of the (3-fluoro)benzyloxy unit to (R)-1 to give (R)-3 led us to determine if this increased activity was associated with the substituted benzyloxyphenyl motif B. Accordingly, we first investigated the Na<sup>+</sup> channel properties of (R)-5 and (S)-5, and the corresponding 4'-aryl extended compound (R)-6. Compounds 5 and 6 contained a 2-amino-3-methylpropionic acid unit in place of the 2-amino-3-methoxypropionic acid moiety found in 1–4.

Macroscopic sodium currents were blocked by (R)-5 almost as effectively as (R)-1 and (R)-2,<sup>22,23</sup> and (R)-6 was more potent than (R)-5 (Figure 6A, B). Compared to control cells, peak macroscopic sodium currents were inhibited by  $\sim 72\%$  by (R)-5 (200  $\mu$ M) and  $\sim 74\%$  by (R)-6 (30  $\mu$ M) (Figure 6B). Neither (R)-5 nor (S)-5 greatly affected the extent of slow inactivation (Figure 6C, D), while the corresponding 4'-aryl extended compound (R)-6 displayed robust slow inactivation at a concentration even 5-fold lower than that employed for both enantiomers of 5. The lack of Na<sup>+</sup> channel slow inactivation for 5 was not surprising despite the excellent antiseizure properties provided by (R)-5 (Table 1). Previous anticonvulsant structure–activity relationship (SAR) studies indicated that the C(2)-hydrocarbon amino acid derivatives, such as (R)-5, likely interacted differently with receptors or at different receptors that control neuronal hyperexcitability than (R)-2, and possibly (R)-1.<sup>11,12,32</sup> As with compounds (R)-1–(R)-4, an analysis of  $V_{1/2}$  and  $k$  values derived from the Boltzmann fits showed that there were no changes in the steady-state activation properties of Na<sup>+</sup> currents between CAD cells treated with DMSO control or the highest concentrations of (R)-5, (S)-5, and (R)-6 (Figure 6E). Steady-state, fast inactivation curves of Na<sup>+</sup> currents from DMSO- and (R)-5-, (S)-5-, and (R)-6-treated CAD cells were well fitted with a single Boltzmann function ( $R^2 > 0.9914$  for all three conditions). Compared with the  $\sim 18.1$  mV shift in  $V_{1/2}$  of fast inactivation in the hyperpolarizing direction observed in the presence of (R)-4 (30  $\mu$ M), the shifts caused by the other agents were minimal: 0.8 mV, (R)-5 (500  $\mu$ M;  $n = 8$ ); 0.9 mV, (S)-5 (500  $\mu$ M;  $n = 7$ ); and 0.9 mV, (R)-6 (100  $\mu$ M;  $n = 3$ ; Figure 6E) ( $p < 0.05$  vs DMSO control; Student's *t* test). In contrast, the excitability of DRGs was inhibited in an enantioselective fashion by 100  $\mu$ M (R)-5 but not (S)-5. As with the slow inactivation, the corresponding 4'-aryl extended compound (R)-6 (100  $\mu$ M) also inhibited excitability compared to DMSO control (Figure 6F;  $p < 0.05$  vs DMSO control, Student's *t* test). We have attributed the pronounced Na<sup>+</sup> channel properties of (R)-6 to the presence of the (3-fluoro)benzyloxyphenyl pharmacophore in this compound.

Next, we explored the electrophysiological properties associated with the (3-fluoro)benzyloxyphenyl unit found in 3, 4, and (R)-6. Thus, we tested (3-fluoro)benzyl phenyl ether (7), 4-((3'-fluoro)benzyloxy)benzylamine (8),<sup>10</sup> and *N*-4-((3'-fluoro)benzyloxy)benzyl acetamide (9).<sup>10</sup> These three compounds contain a substituted benzyloxyphenyl B group but are devoid of the adjacent amino acid unit.

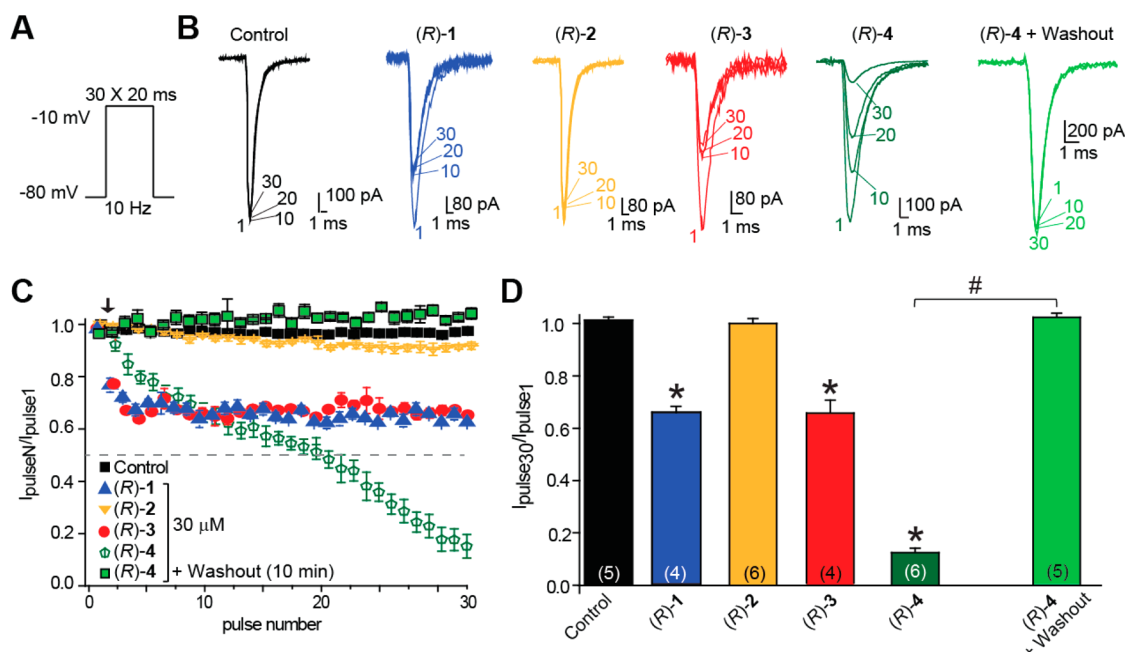


**Figure 4.** Frequency-dependent block of CAD cell  $\text{Na}^+$  currents by selected compounds. (A) The frequency dependence of block was examined by holding cells at the hyperpolarized potential of  $-80$  mV and evoking currents at  $10$  Hz by  $20$  ms test pulses to  $-10$  mV. (B) Representative overlaid traces are illustrated by pulses 1, 10, 20, and 30 for control (predrug) and in the presence of  $30 \mu\text{M}$  (R)-1, (R)-2, (R)-3, and (R)-4. Traces for (R)-4 following a series of three washes (2 mL each) in extracellular bath solution over a 10 min period are also shown. (C) Summary of average frequency-dependent decrease in current amplitude ( $\pm$ SEM) produced by the indicated compounds but not by control conditions. (D) Summary of the maximal decrement in current amplitude observed at the end of the 30-pulse train for predrug (control) and  $30 \mu\text{M}$  (R)-1, (R)-2, (R)-3, and (R)-4. (R)-1, (R)-3, and (R)-4 showed a significant decrease in current amplitude compared with control (\*,  $p < 0.05$ , one-way ANOVA with Dunnett's posthoc test). Note the rapid frequency-dependent facilitation of block by (R)-1, (R)-3, and (R)-4 that was observed beginning as early as pulse 2 (arrow). Washout of cells incubated with  $30 \mu\text{M}$  (R)-4 led to a complete elimination of use-dependence (#,  $p > 0.05$ , one-way ANOVA with Dunnett's posthoc test). Numbers in parentheses are the number of cells patched per condition.

We observed that the (3-fluoro)benzyloxyphenyl units in 7–9 induced almost similar levels of maximal  $\text{Na}^+$  channel slow inactivation (Figure 7A, B) with maximal slow inactivation  $\text{IC}_{50}$  values of  $2.3 \mu\text{M}$  for 7,  $10 \mu\text{M}$  for 8, and  $11.9 \mu\text{M}$  for 9 (Table 1). Again, as with compounds (R)-1–(R)-4, an analysis of  $V_{1/2}$  and  $k$  values derived from the Boltzmann fits showed that there were no changes in the steady-state activation properties of  $\text{Na}^+$  currents between CAD cells treated with DMSO control or the highest concentrations of 7–9 (Figure 7C). Steady-state, fast inactivation curves of  $\text{Na}^+$  currents from DMSO- and 7–9-treated CAD cells were well fitted with a single Boltzmann function ( $R^2 > 0.9908$  for all three conditions). Compared with the  $\sim 18.1$  mV shift in  $V_{1/2}$  of fast inactivation in the hyperpolarizing direction observed in the presence of (R)-4 ( $30 \mu\text{M}$ ), the shifts caused by the other agents were  $17.9$  mV, 7 ( $100 \mu\text{M}$ ;  $n = 4$ );  $18$  mV, 8 ( $100 \mu\text{M}$ ;  $n = 6$ ); and  $12.1$  mV, 9 ( $100 \mu\text{M}$ ;  $n = 6$ , Figure 7C) ( $p < 0.05$  vs DMSO control; Student's  $t$  test). We tested compounds 7 and 8 at a concentration of  $100 \mu\text{M}$ , and observed notable frequency (use)-dependent blockage of  $\text{Na}^+$  currents by the 10th pulse (data not shown). Finally, robust inhibition of the excitability of DRGs was observed with  $100 \mu\text{M}$  of 7–9 ( $p < 0.05$  vs DMSO control; Student's  $t$  test; Figure 7D). Collectively, these results indicated that the (3-fluoro)benzyloxyphenyl unit promoted frequency-dependency blockage of currents and a slow inactivation conformational change in  $\text{Na}^+$  channels.

**Modulation of  $\text{hNa}_V1.1$  by (R)-2 and (R)-4.** We found that while both (R)-2 and (R)-4 displayed exceptional anticonvulsant activity in the MES test (Table 1, MES  $\text{ED}_{50}$  (mg/kg, mice, ip): (R)-2, 4.5; (R)-4, 13), the CAD slow

inactivation  $\text{IC}_{50}$  value for (R)-4 was 400-fold lower (more potent) than (R)-2 (Table 1, maximal slow inactivation  $\text{IC}_{50}$  at  $+20$  mV ( $\mu\text{M}$ ): (R)-2, 120; (R)-4, 0.30). Several factors may account for the lack of correlation of the whole animal anticonvulsant data with the CAD cellular electrophysiological data. One of these is that CAD cells are likely composed of  $\text{Na}_V1.7$ ,  $\text{Na}_V1.1$ , and  $\text{Na}_V1.3$  channels, where  $\text{Na}_V1.7$  mRNA is expressed at 15- and 30-fold higher levels compared with mRNA levels of  $\text{Na}_V1.1$  and  $\text{Na}_V1.3$ , respectively.<sup>23</sup>  $\text{Na}_V1.7$  is highly expressed in the peripheral nervous system and not in the central nervous system (CNS).<sup>30,31</sup>  $\text{Na}_V1.1$  mutations have been linked to generalized epilepsy with febrile seizures, as well as severe myoclonic epilepsy of infancy;<sup>33</sup> therefore, we next asked if (R)-2 and (R)-4 could affect slow inactivation of this channel, and if the slow inactivation  $\text{IC}_{50}$  values for this CNS  $\text{Na}^+$  channel isoform would parallel the observed MES  $\text{ED}_{50}$  values. As there is no selective blocker for  $\text{Na}_V1.3$ , we could not isolate  $\text{Na}_V1.1$  in CAD cells, and instead chose to determine the electrophysiological properties of (R)-2 and (R)-4 on  $\text{hNa}_V1.1$  stably expressed in human embryonic kidney 293 (HEK293) cells.

Compound (R)-4, which has both a 4'-(3-fluoro)-benzyloxyphenyl substituent and a *N*-acetyl moiety, demonstrated a higher extent of slow inactivation than (R)-2 at both  $-50$  mV and at  $+20$  mV (a voltage at which maximal slow inactivation was observed) (Figure 8C–F). The maximal slow inactivation  $\text{IC}_{50}$  at  $+20$  mV was 120-fold lower with (R)-4 ( $4 \mu\text{M}$ ) compared with (R)-2 ( $480 \mu\text{M}$ ); the activation and fast-inactivation properties of  $\text{Na}_V1.1$  were not affected by the compounds (Figure 8G). We also examined the rate time

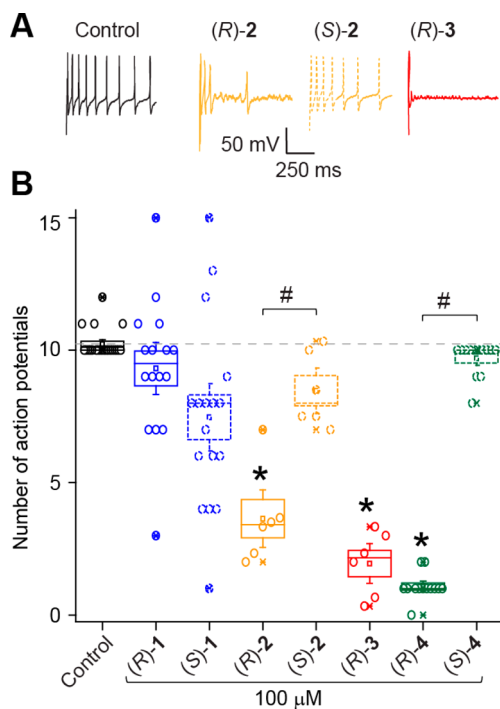


**Figure 5.** DRG neuronal excitability following application of *N*-benzyl 2-amino-3-methoxypropionamide derivatives. (A) Representative recordings of medium diameter DRG neuronal firing before and during application of compounds (R)-2, (S)-2, and (R)-3. Neuronal excitability is significantly decreased following 100  $\mu\text{M}$  (R)-2, (R)-3, and (R)-4, but not (S)-2. (B) Group data. Box plots (with overlapping data points representing number of action potentials from each cell) showing mean number of action potentials  $\pm$  SEM elicited by current injection in medium diameter DRG neurons during baseline control conditions and in the presence of 100  $\mu\text{M}$  of the indicated compounds. Asterisks indicate statistically significant differences in fraction of current available between predrug (control) and (R) compounds (\*,  $p < 0.05$ , one-way ANOVA with Dunnett's posthoc test). Hash mark indicates a statistically significant difference in fraction of current available between (R)- and (S)-enantiomers. For all experiments, data are from 8–11 cells per condition from at least three different rats.

course of block development by these agents. Block development was examined by holding the cells at  $-120$  mV in the absence or presence of 100  $\mu\text{M}$  (R)-2 or (R)-4, prepulsing the cells to 0 mV for varying amounts of time to allow block to develop, hyperpolarizing the cells to  $-120$  mV for 20 ms to allow unbound channels to recover from fast inactivation, then stepping the cells to 0 mV for 20 ms to determine the fraction of channels available for activation (Figure 8H). The reduction in the fraction of current available is indicative of the time course for the development of slow inactivation. The time course for reducing channel availability without drug, as well as in the presence of (R)-2 and (R)-4, was biphasic, with a fast component likely representing block development of fast-inactivated channels and a slow component consistent with the time course of slow inactivation development (Figure 8H). The time constant for block development was  $\sim 25$ -fold faster in cells treated with (R)-4 (100  $\mu\text{M}$ ) compared with vehicle- or (R)-2 (100  $\mu\text{M}$ )-treated cells. (R)-4 significantly reduced the fraction of current at all times between 50 and 8000 ms (Figure 8H) compared with control or (R)-2-treated cells ( $p < 0.05$ , one-way ANOVA with Dunnett's posthoc test). Finally, we tested if (R)-2 and (R)-4, could elicit frequency-dependent

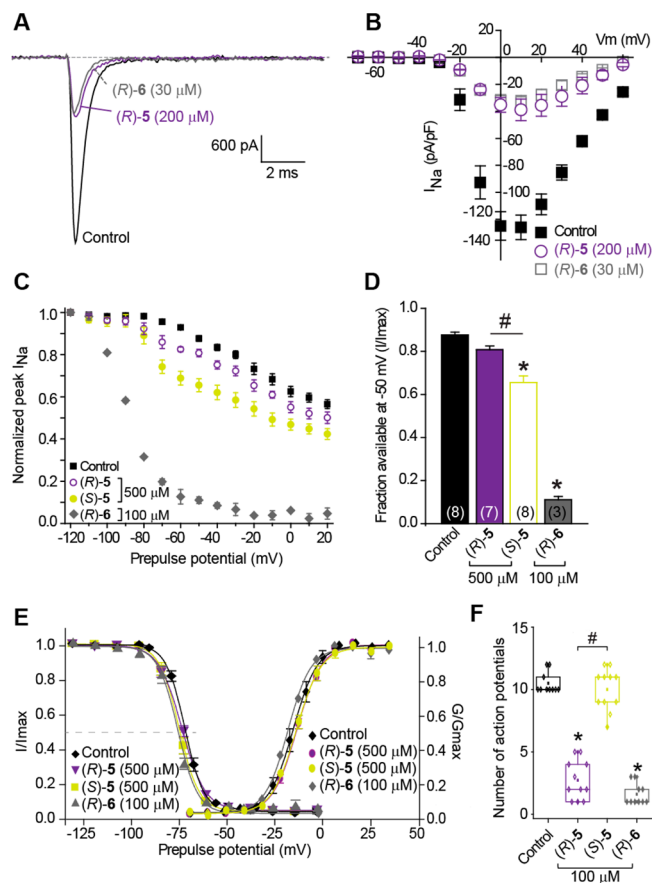


**Figure 6.** Effects of *N*-benzyl 2-amino-3-methylpropionamides (R)-5 and (S)-5, and the corresponding 4'-aryl extended derivative (R)-6 on slow inactivation, activation, and fast-inactivation of  $\text{Na}^+$  currents in CAD cells, and firing properties of sensory neurons. (A) Representative peak  $\text{Na}^+$  current responses, evoked by a step to 0 mV from a holding potential of  $-80$  mV, of CAD cells treated with 0.5% DMSO (control), 200  $\mu\text{M}$  (R)-5, or 30  $\mu\text{M}$  (R)-6. (B) Summary of current–voltage ( $I$ – $V$ ) relationships for CAD cells treated with the compounds illustrated in A ( $n = 3$ –5 each). (C) Summary of steady-state, slow inactivation curves for CAD cells treated with DMSO (control), 500  $\mu\text{M}$  (R)-5 and (S)-5, or 100  $\mu\text{M}$  (R)-6. Some drug-induced slow inactivation was apparent in CAD cells treated with (S)-5 with more pronounced slow inactivation observed with (R)-6, while almost no slow inactivation was observed with (R)-5. Some error bars are smaller than the symbols. (D) Summary of the fraction of current available at  $-50$  mV for CAD cells in the absence or presence of (R)- or (S)-enantiomers of the indicated compounds. Asterisks indicate statistically significant differences in fraction of current available between predrug and (R)- and (S)-compounds ( $p < 0.05$ , one-way ANOVA with Dunnett's posthoc test). Hash mark indicates a statistically significant difference in fraction of current available between (R)- and (S)-enantiomers. Numbers in parentheses are the number of cells patched per condition. The half-maximal values for slow inactivation for these compounds are shown in Table 1. (E) Values for  $V_{1/2}$ , the voltage of half-maximal activation or inactivation, were derived from Boltzmann distribution fits to the individual recordings and averaged to determine the mean ( $\pm$ SEM) voltage dependence of activation or inactivation, respectively. The voltage protocol used to evoke current responses is shown above the curves. Representative Boltzmann fits for 0.1–1% DMSO (control) and various concentrations of the compounds are shown. The  $V_{1/2}$  and  $k$  (slope; not shown) of activation were not different among any of the compounds tested ( $p > 0.05$ , one-way ANOVA). All compounds induced a  $\sim 8$  mV hyperpolarizing shift in the  $V_{1/2}$  of fast inactivation. For all experiments, data are from 6–9 cells per condition. F. Box plots

Figure 6. continued

(with overlapping data points representing number of action potentials from each cell) showing mean number of action potentials  $\pm$  SEM elicited by current injection in medium diameter DRG neurons during baseline control conditions and in the presence of 100  $\mu$ M of the indicated compounds. Asterisks indicate statistically significant differences in fraction of current available between predrug (control) and (R) compounds (\*,  $p < 0.05$ , one-way ANOVA with Dunnett's posthoc test). Hash mark indicates a statistically significant difference in fraction of current available between (R)- and (S)-enantiomers. For these experiments, data are from 8–11 cells per condition from at least two different rats.

block. A train of 30 test pulses (20 ms to  $-10$  mV) was delivered from a holding potential of  $-80$  mV at 10 Hz (Figure 8I). The available current in control cells and cells in the presence of the compounds was calculated by dividing the peak current at any given pulse (pulse<sub>N</sub>) by the peak current in response to the initial pulse (pulse<sub>1</sub>). Both (R)-2 and (R)-4 did not reduce current amplitude compared with control (Figure 8I, J). Our results point to the potent activity of (R)-4 on slow inactivation of Na<sub>v</sub>1.1 channels.

## CONCLUSION

In this study, we asked if the cellular pharmacology for compounds 1–4 was similar. We focused on the Na<sup>+</sup> channel because the AED (R)-2 and the 4'-aryl-extended compound (R)-4 have been shown to facilitate entry of Na<sup>+</sup> channels into the slow inactivation state.<sup>15–17,22,23</sup> Compounds 1–4 affected Na<sup>+</sup> channel slow inactivation, but the extent of slow inactivation and the stereoselectivity for slow inactivation was markedly affected by terminal amine acetylation and extension of the 4'-aryl group (Figure 2). Compound (R)-4 was the most potent Na<sup>+</sup> channel modulator; it was 390-fold more effective in inducing maximal Na<sup>+</sup> channel slow inactivation (at +20 mV) than (R)-2. Moreover, (R)-4 was 1100-fold more active than its stereoisomer (S)-4. By comparison, (R)-2 was only >21-fold more active than (S)-2 in inducing Na<sup>+</sup> channel slow inactivation. Our findings indicated that the pronounced activity and stereoselectivity of (R)-4 was uniquely influenced by a combination of the *N*-acetyl and the (3-fluoro)-benzyloxyphenyl structural units, and where the concurrent incorporation of both groups contributed to its Na<sup>+</sup> channel slow inactivation activity. We also found that the 4'-aryl extended compounds (R)-3 and (R)-4 exhibited frequency (use)-dependent inhibition of Na<sup>+</sup> currents. Frequency-dependent block is a powerful way to control neuronal hyperexcitability in rapidly firing neurons.

Since the extended 4'-aryl substituent in (R)-4 significantly increased Na<sup>+</sup> channel slow inactivation, we determined the Na<sup>+</sup> channel properties of (R)-6 and 7–9, and documented that the (3-fluoro)benzyloxyphenyl moiety in these compounds contributed to their observed Na<sup>+</sup> channel slow inactivation properties (maximal slow inactivation IC<sub>50</sub> at +20 mV ( $\mu$ M): (R)-6, 0.60; 7, 2.3; 8, 10; 9, 12) (Table 1). Moreover, we showed that 7 and 8 inhibited Na<sup>+</sup> currents in a frequency (use)-dependent manner. Collectively, our findings indicated that the substituted benzyloxyphenyl unit B is an effective pharmacophore for modulating Na<sup>+</sup> channel function and provides a structural unit for the design of neurological agents targeting these channels. Importantly, our earlier SAR studies<sup>10</sup> demonstrated that considerable structural latitude exists for the

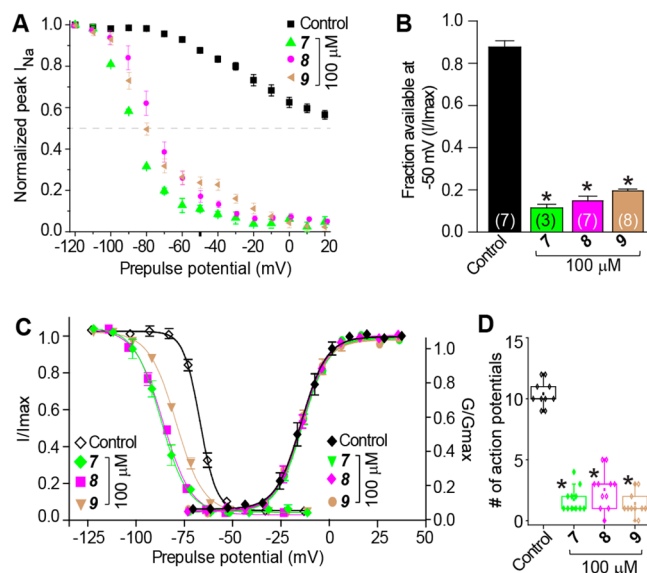


**Figure 7.** Effects of the substituted benzyloxyphenyl motif B without the adjacent amino acid unit in compounds 7–9 on slow inactivation, activation, and fast-inactivation of Na<sup>+</sup> currents in CAD cells, and firing properties of sensory neurons. (A) Summary of steady-state, slow inactivation curves for CAD cells treated with DMSO (control) or 100  $\mu$ M of 7–9. Robust drug-induced slow inactivation was apparent in CAD cells treated with compounds 7–9. Some error bars are smaller than the symbols. (B) Summary of the fraction of current available at  $-50$  mV for CAD cells in the absence or presence of compounds 7–9. Asterisks indicate statistically significant differences in fraction of current available between predrug and compounds 7–9 ( $p < 0.05$ , one-way ANOVA with Dunnett's posthoc test). Numbers in parentheses are the number of cells patched per condition. The half-maximal values for slow inactivation for these compounds are shown in Table 1. (C) Values for  $V_{1/2}$ , the voltage of half-maximal activation or inactivation, were derived from Boltzmann distribution fits to the individual recordings and averaged to determine the mean ( $\pm$ SEM) voltage dependence of activation or inactivation, respectively. The voltage protocol used to evoke current responses is shown above the curves. Representative Boltzmann fits for 0.1–1% DMSO (control) and various concentrations of the compounds are shown. The  $V_{1/2}$  and  $k$  (slope; not shown) of activation were not different among any of the compounds tested ( $p > 0.05$ , one-way ANOVA). The compounds induced a  $\sim 12$ – $18$  mV hyperpolarizing shift in the  $V_{1/2}$  of fast inactivation. For all experiments, data are from 5–9 cells per condition. (D) Box plots (with overlapping data points representing number of action potentials from each cell) showing the mean number of action potentials  $\pm$  SEM elicited by current injection in medium diameter DRG neurons during baseline control conditions and in the presence of 100  $\mu$ M of the indicated compounds. Asterisks indicate statistically significant differences in fraction of current available between predrug (control) and compounds 7–9 (\*,  $p < 0.05$ , one-way ANOVA with Dunnett's posthoc test). For these experiments, data are from 8–11 cells per condition from at least 2 different rats.

4'-aryl-extended unit in compounds such as 3, 4, and 6, and that these compounds exhibited excellent Na<sup>+</sup> channel slow and, in some cases, fast inactivation properties.<sup>22</sup> Currently, we are exploring the utility of this general pharmacophore unit for the design of novel neurological agents.

We tested the effects of (R)-2 and (R)-4 on hNa<sub>v</sub>1.1 stably expressed in HEK293 cells. We found that (R)-4 was 120-fold more effective than (R)-2 in transitioning Na<sup>+</sup> channels to the slow inactivation state (maximal slow inactivation IC<sub>50</sub> at +20 mV ( $\mu$ M): (R)-2, 480; (R)-4, 4). A similar pattern was observed in CAD cells, where approximately 50% of the Na<sup>+</sup>

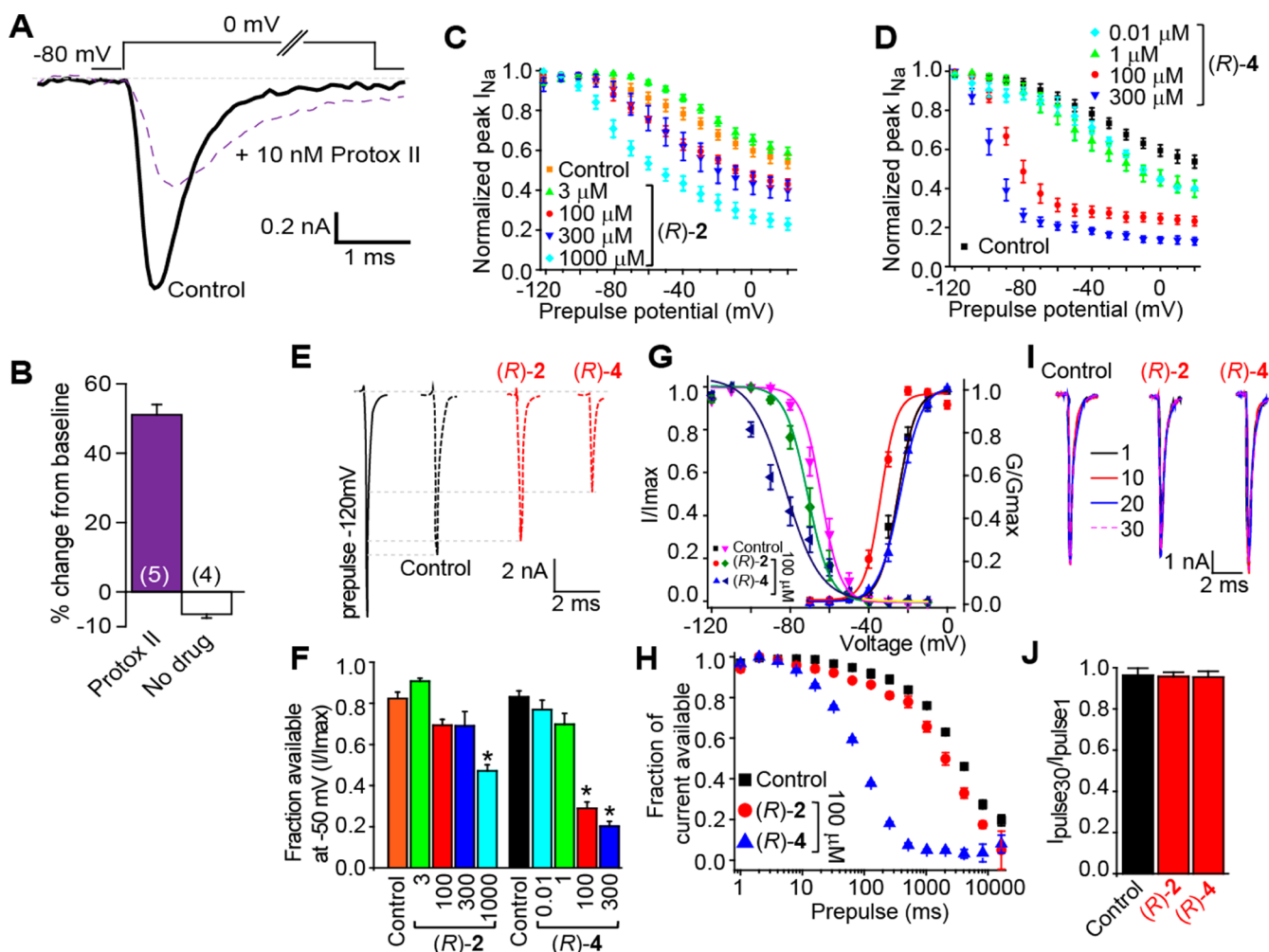


**Figure 8.** Analysis of *N*-benzyl 2-acetamido-3-methoxypropionamide ((*R*)-2) and the 4'-(3-fluoro)benzyloxy derivative ((*R*)-4) on electrophysiological properties of  $\text{Na}_V1.1$  currents in HEK293 cells. (A) Representative current traces from CAD cells in the absence (control) or presence of the  $\text{Na}_V1.1$ -selective blocker prototox II (10 nM) in response to a voltage step from  $-80$  to  $0$  mV for 200 ms. In the example shown, the peak current decreased by  $\sim 50\%$  from a control value of  $1472.6$  pA to a value of  $739.85$  pA 15 min postapplication of prototox II (10 nM). (B) Summary of the mean  $\pm$  SEM change in current relative to the current at 4 min following acquisition of whole cell (baseline) for 10 nM prototox II ( $n = 5$ ) and control. There was a small buildup in current density in control cells ( $n = 4$ ). The rest of the figure describes data from HEK293 cells stably transfected with  $\text{Na}_V1.1$  (C–J). Steady-state, slow inactivation curves for HEK293 cells expressing wildtype h $\text{Na}_V1.1$  in response to a range of concentrations of (*R*)-2 (C) or (*R*)-4 (D). Voltage protocol for assessing slow inactivation is as described in the legend to Figure 1. (E) Representative current traces at  $-50$  mV from cells that underwent no treatment, or treatment with  $100 \mu\text{M}$  (*R*)-2, and  $100 \mu\text{M}$  (*R*)-4. As a comparator of the extent of slow inactivation, a control trace at  $-120$  mV (prepulse) is also shown. (F) Summary of steady-state, slow inactivation curves for  $\text{Na}_V1.1$  HEK293 cells treated with DMSO (control), or various concentrations of (*R*)-2 or (*R*)-4. (G) Fast inactivation curves for  $\text{Na}_V1.1$  HEK293 cells in response to no treatment (control),  $100 \mu\text{M}$  (*R*)-2, and  $100 \mu\text{M}$  (*R*)-4. The curves are derived from Boltzmann distribution fits to the individual recordings and averaged to determine the mean ( $\pm$ SEM) of steady-state inactivation ( $I/I_{\text{max}}$ ). Voltage protocol for fast inactivation stepped from  $-120$  to  $-10$  mV in 10 mV increments for a pulse duration of 500 ms. Fraction of channels available was then measured at 0 mV. Activation curves for the no treatment (control),  $100 \mu\text{M}$  (*R*)-2, and  $100 \mu\text{M}$  (*R*)-4 were normalized to  $G/G_{\text{max}}$  and curves were derived from Boltzmann distribution fits as previously described. The voltage protocol for steady-state activation stepped from  $-80$  mV to  $0$  mV. (H)  $\text{Na}_V1.1$  HEK293 cells were held at  $-120$  mV, depolarized to  $0$  mV for 10 ms or 5 s, and then hyperpolarized to  $-120$  mV for varying increasing durations before testing the available current with a step depolarization to  $0$  mV. Data sweeps were acquired at 0.5 Hz for short recovery durations and at slower rates for the longer recovery durations. (*R*)-4 caused a pronounced decrease in the rate of inactivation/inhibition recovery (by the 10 ms prepulse) for  $\text{Na}^+$  channels, whereas (*R*)-2 had no effect. (I) The frequency dependence of block was examined by holding cells at the hyperpolarized potential of  $-80$  mV and evoking currents at 10 Hz by 20 ms test pulses to  $-10$  mV. Representative overlaid traces are illustrated by pulses 1, 10, 20, and 30 for control (predrug) and in the presence of (*R*)-2 and (*R*)-4. (J) Summary of average frequency-dependent decrease in current amplitude ( $\pm$ SEM) produced by no treatment (control), (*R*)-2 or (*R*)-4. Neither compound induced use (\*,  $p > 0.05$ , one-way ANOVA with Dunnett's posthoc test).

current can be attributed to  $\text{Na}_V1.7$  channels (maximal slow inactivation  $\text{IC}_{50}$  at  $+20$  mV ( $\mu\text{M}$ ): (*R*)-2, 120; (*R*)-4, 0.30).<sup>22</sup> The enhanced  $\text{Na}^+$  channel activity for (*R*)-4 versus (*R*)-2 differs from their MES anticonvulsant activities, where (*R*)-2 is  $\sim 3$ -fold more potent than (*R*)-4 in mice (i.p.). Thus, other

factors (e.g., pharmacokinetics) may be partially responsible for the observed anticonvulsant activities. These results underscore the importance of conducting both cellular electrophysiology and in vivo testing in drug screening protocols designed to identify new neurological agents.

Finally, we learned that the C(2)-hydrocarbon compound (R)-5, despite its structural similarity to (R)-1 and (R)-2, did not modulate Na<sup>+</sup> channel slow inactivation activity. The antiepileptic activity of (R)-2 has been attributed to its ability to promote Na<sup>+</sup> channel slow inactivation.<sup>15–17,23</sup> Nonetheless, (R)-5 exhibited pronounced anticonvulsant activity in the MES test (ED<sub>50</sub> = 15 mg/kg, mice (ip)). These findings provide an instructive example of how molecules that share common structural features can either interact differently with receptors or with a different set of receptors that control neuronal hyperexcitability and still show pronounced efficacy in the same animal model.

## METHODS

**Materials.** Synthetic procedures and analytical characterization for compounds 1, 2, (R)-3, 4, 5, (R)-6, 8, and 9 have been previously reported.<sup>6,10–12</sup> Compound 7 was purchased from Sigma.

**Catecholamine A Differentiated (CAD) Cells.** CAD cells were grown at 37 °C and in 5% CO<sub>2</sub> (Sarstedt, Newton, NC) in Ham's F12/EMEM medium (GIBCO, Grand Island, NY), supplemented with 8% fetal bovine serum (FBS; Sigma, St. Louis, MO) and 1% penicillin/streptomycin (100% stocks, 10 000 U/mL penicillin G sodium and 10 000 µg/mL streptomycin sulfate).<sup>22,23,34</sup> Cells were passaged every 6–7 days at a 1:25 dilution.

**Human Embryonic Kidney 293 (HEK293) Cells Expressing Na<sub>v</sub>1.1.** A codon-optimized synthetic gene encoding the human Na<sub>v</sub>1.1 (wild-type) channel open reading frame (NC\_000002.11) was transfected into HEK293 cells using the calcium phosphate precipitation technique. After 48 h, the cells were passaged into 100 mm dishes and treated with G418 (Geneticin, Life Technologies) at 800 µg/µL to select for neomycin resistant cells. After 2 weeks, colonies were picked and split. The colonies were then tested for channel expression with whole-cell patch-clamp technique. The cell line was then maintained with 500 µg/µL G418. Na<sub>v</sub>1.1 stable cell line was grown under standard tissue culture conditions (5% CO<sub>2</sub> at 37 °C) in Dulbecco's modified Eagle's medium supplemented with 10% fetal bovine serum.

**Whole-Cell Patch Clamp.** Whole-cell patch clamp recordings were performed at room temperature on CAD cells using an EPC 10 Amplifier (HEKA Electronics, Germany) as described previously.<sup>22,23</sup> Electrodes were pulled from thin-walled borosilicate glass capillaries (Warner Instruments, Hamden, CT) with a P-97 electrode puller (Sutter Instrument, Novato, CA) such that final electrode resistances were 1–2 MΩ when filled with internal solutions. The internal solution for recording Na<sup>+</sup> currents contained (in mM): 110 CsCl, 5 MgSO<sub>4</sub>, 10 EGTA, 4 ATP Na<sub>2</sub>-ATP, 25 Hepes (pH 7.2, 290–310 mOsm/L). The external solution contained (in mM) 100 NaCl, 10 tetraethylammonium chloride (TEA-Cl), 1 CaCl<sub>2</sub>, 1 CdCl<sub>2</sub>, 1 MgCl<sub>2</sub>, 10 D-glucose, 4 4-AP, 0.1 NiCl<sub>2</sub>, and 10 Hepes (pH 7.3, 310–315 mOsm/L). Whole-cell capacitance and series resistance were compensated with the amplifier. Series resistance error was always compensated to be less than ±3 mV. Cells were considered only when the seal resistance was less than 3 MΩ. Linear leak currents were digitally subtracted by P/4.

Na<sup>+</sup> channel fast- and slow-inactivated states were induced as previously described.<sup>22,23</sup> For fast inactivation, cells were held at –80 mV, stepped to inactivating prepulse potentials ranging from –120 to –10 mV (in 10 mV increments) for 500 ms, and then the cells were stepped to 0 mV for 20 ms to measure the available current. A 500 ms conditioning pulse was used because it allowed all endogenous channels to transition to a fast-inactivation state at all potentials assayed. For slow inactivation, CAD cells were held at –80 mV and conditioned to potentials ranging from –120 to +20 mV (in 10 mV increments) for 5 s. Then, fast-inactivated channels were allowed to recover for 150 ms at a hyperpolarized pulse to –120 mV, and the fraction of channels available was tested by a single depolarizing pulse to 0 mV for 15 ms. This brief hyperpolarization allowed the channels to recover from fast inactivation while limiting recovery from slow

inactivation. Using this protocol, a series of compound response curves were generated showing the normalized peak ( $I_{Na}$ ) versus prepulse potential (mV) at a given compound concentration.

**Data Acquisition and Analysis.** Signals were filtered at 10 kHz and digitized at 10–20 kHz. Analysis was performed using Fitmaster and origin8.1 (OriginLab Corporation, Northampton, MA). For activation curves, conductance ( $G$ ) through Na<sup>+</sup> channels was calculated using the equation  $G = I/(V_m - V_{rev})$ , where  $V_{rev}$  is the reversal potential,  $V_m$  is the membrane potential at which the current was recorded, and  $I$  is the peak current. Activation and inactivation curves were fitted to a single-phase Boltzmann function  $G/G_{max} = 1/\{1 + \exp[(V - V_{50})/k]\}$ , where  $G$  is the peak conductance,  $G_{max}$  is the fitted maximal  $G$ ,  $V_{50}$  is the half activation voltage, and  $k$  is the slope factor. Additional details of specific pulse protocols are described in the results text or figure legends.

**Animals.** Pathogen-free, adult female Sprague–Dawley rats (150–200 g; Harlan Laboratories, Madison, WI) were housed in temperature (23 ± 3 °C) and light (12 h light: 12 h dark cycle; lights on at 07:00 h) controlled rooms with standard rodent chow and water available ad libitum. Experiments were performed during the light cycle. These experiments were approved by the Institutional Animal Care and Use Committee of Indiana University/Purdue University in Indianapolis. All procedures were conducted in accordance with the Guide for Care and Use of Laboratory Animals published by the National Institutes of Health and the ethical guidelines of the International Association for the Study of Pain. All animals were randomly assigned to either treatment or control groups.

**Preparation of Acutely Dissociated Dorsal Root Ganglion Neurons.** The L1–L6 DRGs were acutely dissociated using methods described by Ma and LaMotte.<sup>35</sup> Briefly, L1–L6 DRGs were removed from naive Sprague–Dawley rats. The DRGs were treated with collagenase A and collagenase D in HBSS for 20 min (1 mg/mL; Roche Applied Science, Indianapolis, IN), followed by treatment with papain (30 units/mL, Worthington Biochemical, Lakewood, NJ) in HBSS containing 0.5 mM EDTA and cysteine at 35 °C. The cells were then dissociated via mechanical trituration in culture media containing 1 mg/mL bovine serum albumin and trypsin inhibitor (1 mg/mL, Sigma, St. Louis MO). The culture media was DMEM, Ham's F12 mixture, supplemented with 10% fetal bovine serum, penicillin and streptomycin (100 µg/mL and 100 U/mL), N<sub>2</sub> (Life Technologies), and 20 nM NGF (Sigma-Aldrich, St. Louis, MO). The cells were then plated on coverslips coated with poly-L-lysine and laminin (1 mg/mL) and incubated for 2–3 h before more culture media was added to the wells. The cells were then allowed to sit undisturbed for 4–18 h to adhere at 37 °C (with 5% CO<sub>2</sub>).

**Current Clamp Electrophysiology.** Sharp-electrode intracellular recordings were obtained 4–18 h after dissociation using a modified method described by Ma and LaMotte.<sup>35</sup> Coverslips were transferred to a recording chamber that was mounted on the stage of an inverted microscope (Nikon Eclipse Ti, Nikon Instruments Inc., Melville, NY). The chamber was perfused with a bath solution containing (mM): 120 NaCl, 3 KCl, 1 CaCl<sub>2</sub>, 1 MgCl<sub>2</sub>, 10 Hepes, 10 glucose, adjusted to pH 7.4 and osmolarity 300 mOsm. The recordings were obtained at room temperature. Intracellular recording electrodes were fabricated from borosilicate glass (World Precision Instruments, Sarasota, FL) and pulled on a Flaming/Brown micropipet puller (P-98, Sutter Instruments, Novato, CA). Electrodes were filled with 1.0 M KCl (impedance: 40–80 MΩ) and positioned by a micromanipulator (Newport Corporation, Irvine, CA). A –0.1 nA current injection was used to bridge-balance the electrode resistance. Prior to electrode impalement, the size of the soma to be recorded was classified according to its diameter as small (≤30 µm), medium (31–45 µm), and large (≥45 µm). Only medium size neurons were used in these experiments as these neurons consistently exhibited the ability to fire multiple action potentials without accommodation. Electrophysiological recordings were performed with continuous current-clamp in bridge mode using an AxoClamp-2B amplifier, stored digitally via Digidata 1322A interface, and analyzed offline with pClamp 9 software (Axon Instruments, Union City, CA). A neuron was accepted for study only when it exhibited a resting membrane potential more negative

than  $-45$  mV. Action potentials were evoked by injecting current steps of 1 s duration through the intracellular recording electrode from 0.1 nA in increments of 0.1 nA until evoking 8–10 action potentials per current pulse, or reaching 4 nA. Baseline neuronal excitability was measured by injecting 1 s current pulses into the soma every 30 s. Following three control current injections, compounds were applied to the coverslip (final concentration of  $100 \mu\text{M}$ ) and current injections continued every 30 s. Neuronal excitability was measured as number of action potentials elicited per current pulse before and after addition of compounds.

## AUTHOR INFORMATION

### Corresponding Author

\*(H.K.) Mailing address: Division of Chemical Biology and Medicinal Chemistry, UNC Eshelman School of Pharmacy, University of North Carolina, Chapel Hill, North Carolina 27599-7568, and Department of Chemistry, University of North Carolina, Chapel Hill, North Carolina 27599-3290. E-mail: hkohn@email.unc.edu. Telephone: 919-843-8112. Fax: 919-966-0204. (R.K.) Mailing address: Departments of Pharmacology and Toxicology and Program in Medical Neuroscience, Paul and Carole Stark Neurosciences Research Institute, Indiana University School of Medicine, Indianapolis, Indiana 46202. E-mail: khanna5@iupui.edu. Telephone: 317-278-6531.

### Author Contributions

∇ These authors contributed equally to this work.

### Author Contributions

X.-F.Y., Y.W., E.T.D., and A.D.P. conducted whole cell electrophysiology. S.M.W. provided assistance with all cell culture. A.M.K. and C.S. synthesized the compounds. A.M.K. helped construct the paper. C.B. and T.R.C. created the HEK293  $\text{Na}_v1.1$  cell line. M.R.D. performed the current clamp recordings on DRGs. F.A.W. contributed to the writing of the current clamp electrophysiology section. A.M.K., R.K., and H.K. conceived the study. R.K. and H.K. designed and supervised the overall project and wrote the manuscript.

### Funding

This work is supported by grants from a UL1RR025747 award from the National Center for Research Resources (H.K.), a National Scientist Development grant from the American Heart Association (SDG5280023 to R.K.), a Neurofibromatosis New Investigator Award from the Department of Defense Congressionally Directed Military Medical Research and Development Program (NF1000099 to R.K.), the Indiana State Department of Health–Spinal Cord and Brain Injury Fund (A70-9-079138 to R.K.), the Indiana University Biomedical Committee–Research Support Funds (2286501 to R.K.), the Elwert Award in Medicine to R.K., and a grant from National Institute on Drug Abuse (DA026040 to F.A.W.). E.T.D. was supported by a Paul and Carol Stark Medical Neuroscience Fellowship.

### Notes

The content is solely the responsibility of the authors and does not represent the official views of the National Center for Research Resources, National Institute of Neurological Disorders and Stroke, or the National Institutes of Health. The authors declare the following competing financial interest(s): Harold Kohn has a royalty-stake position in (R)-2, and UNC has filed patent applications in behalf of the compounds in this study.

## ACKNOWLEDGMENTS

We thank the National Institute of Neurological Disorders and Stroke and the Anticonvulsant Screening Program at the National Institutes of Health with Drs. Tracy Chen and Jeffrey Jiang, and James P. Stables for kindly performing the pharmacological studies via the Anticonvulsant Screening Program's contract site at the University of Utah with Drs. H. Wolfe, H. S. White, and K. Wilcox.

## ABBREVIATIONS

AED, antiepileptic drug; CAD, catecholamine A differentiated;  $\text{ED}_{50}$ , 50% effective dose; HEK 293, human embryonic kidney 293;  $\text{IC}_{50}$ , concentration at which half of the channels have transitioned to a slow inactivated state;  $I_{\text{Na}}$ ,  $\text{Na}^+$  current; DRG, dorsal root ganglion; ip, intraperitoneally; MES, maximal electroshock seizure;  $\text{Na}_v1.x$ , voltage-gated  $\text{Na}^+$  channel isoform 1.x; po, orally; SAR, structure–activity relationship;  $\text{TD}_{50}$ , 50% neurological impairment; VGSC, voltage-gated  $\text{Na}^+$  channel

## REFERENCES

- (1) Stafstrom, C. E. (2006) Epilepsy: A review of selected clinical syndromes and advances in basic science. *J. Cereb. Blood Flow Metab.* 26, 983–1004.
- (2) Fisher, R. S., Boas, W. v. E., Blume, W., Elger, C., Genton, P., Lee, P., and Engel, J., Jr. (2005) Epileptic seizures and epilepsy: Definitions proposed by the International League Against Epilepsy (ILAE) and the International Bureau for Epilepsy (IBE). *Epilepsia* 46, 470–472.
- (3) Picot, M. C., Baldy-Moulinier, M., Dauris, J. P., Dujols, P., and Crespel, A. (2008) The prevalence of epilepsy and pharmacoresistant epilepsy in adults: A population-based study in a western European country. *Epilepsia* 49, 1230–1238.
- (4) Pellock, J. M., and Willmore, L. J. (1991) A rational guide to monitoring in patients receiving anticonvulsants. *Neurology* 41, 961–964.
- (5) Levy, R. H., Mattson, R., and Meldrum, B. (1995) *Antiepileptic Drugs*, 4th ed., Raven Press, New York.
- (6) Choi, D., Stables, J. P., and Kohn, H. (1996) Synthesis and anticonvulsant activities of *N*-benzyl-2-acetamidopropionamide derivatives. *J. Med. Chem.* 39, 1907–1916.
- (7) Andurkar, S. V., Stables, J. P., and Kohn, H. (1998) Synthesis and anticonvulsant activities of (R)-(O)-methylserine derivatives. *Tetrahedron: Asymmetry* 9, 3841–3854.
- (8) Béguin, C., LeTiran, A., Stables, J. P., Voyksner, R. D., and Kohn, H. (2004) *N*-Substituted amino acid *N'*-benzylamides: Synthesis, anticonvulsant, and metabolic activities. *Bioorg. Med. Chem.* 12, 3079–3096.
- (9) Salomé, C., Salomé-Grosjean, E., Park, K. D., Morieux, P., Swendiman, R., DeMarco, E., Stables, J. P., and Kohn, H. (2010) Synthesis and anticonvulsant activities of (R)-*N*-(4'-substituted)benzyl 2-acetamido-3-methoxypropionamides. *J. Med. Chem.* 53, 1288–1305.
- (10) Salomé, C., Salomé-Grosjean, E., Stables, J. P., and Kohn, H. (2010) Merging the structural motifs of functionalized amino acids and  $\alpha$ -aminoamides: Compounds with significant anticonvulsant activities. *J. Med. Chem.* 53, 3756–3771.
- (11) King, A. M., Salomé, C., Dinsmore, J., Salomé-Grosjean, E., De Ryck, M., Kaminski, R., Valade, A., and Kohn, H. (2011) Primary amino acid derivatives: Compounds with anticonvulsant and neuropathic pain protection activities. *J. Med. Chem.* 54, 4815–4830.
- (12) King, A. M., Salomé, C., Salomé-Grosjean, E., De Ryck, M., Kaminski, R., Valade, A., Stables, J. P., and Kohn, H. (2011) Primary amino acid derivatives: Substitution of the 4'-*N'*-benzylamide site in (R)-*N'*-benzyl 2-amino-3-methylbutanamide, (R)-*N'*-benzyl 2-amino-3,3-dimethylbutanamide, and (R)-*N'*-benzyl 2-amino-3-methoxypropionamide provides potent anticonvulsants with pain attenuating properties. *J. Med. Chem.* 54, 6417–6431.

- (13) Porter, R. J., Cereghino, J. J., Gladding, G. D., Hessie, B. J., Kupferberg, H. J., Scoville, B., and White, B. G. (1984) Antiepileptic Drug Development Program. *Cleveland Clin. Q.* 51, 293–305.
- (14) Perucca, E., Yasothan, U., Clincke, G., and Kirkpatrick, P. (2008) Lacosamide. *Nat. Rev. Drug Discovery* 7, 973–974.
- (15) Errington, A. C., Stöhr, T., Heers, C., and Lees, G. (2008) The investigational anticonvulsant lacosamide selectively enhances slow inactivation of voltage-gated sodium channels. *Mol. Pharmacol.* 73, 157–169.
- (16) Sheets, P. L., Heers, C., Stöhr, T., and Cummins, T. R. (2008) Differential block of sensory neuronal voltage-gated sodium channels by lacosamide [(2R)-2-(acetylamino)-N-benzyl-3-methoxypropanamide], lidocaine, and carbamazepine. *J. Pharmacol. Exp. Ther.* 326, 89–99.
- (17) Wang, Y., Brittain, J. M., Jarecki, B. W., Park, K. D., Wilson, S. M., Wang, B., Hale, R., Meroueh, S. O., Cummins, T. R., and Khanna, R. (2010) In silico docking and electrophysiological characterization of lacosamide binding sites on collapsin response mediator protein-2 identifies a pocket important in modulating sodium channel slow inactivation. *J. Biol. Chem.* 285, 25296–25307.
- (18) Costigan, M., Scholz, J., and Woolf, C. (2009) Neuropathic pain: a maladaptive response of the nervous system to damage. *Annu. Rev. Neurosci.* 32, 1–32.
- (19) Beyreuther, B. K., Freitag, J., Heers, C., Krebsfanger, N., Scharfenecker, U., and Stöhr, T. (2007) Lacosamide: A review of preclinical properties. *CNS Drug Rev.* 13, 21–42.
- (20) Dickinson, T., Lee, K., Spanswick, D., and Munro, F. E. (2003) Leading the charge—pioneering treatments in the fight against neuropathic pain. *Trends Pharmacol. Sci.* 24, 555–557.
- (21) Dickenson, A. H., Matthews, E. A., and Suzuki, R. (2002) Neurobiology of neuropathic pain: Mode of action of anticonvulsants. *Eur. J. Pain* 6 (Suppl. A), 51–60.
- (22) Wang, Y., Wilson, S. M., Brittain, J. M., Ripsch, M. S., Salomé, C., Park, K. D., White, F. A., Khanna, R., and Kohn, H. (2011) Merging structural motifs of functionalized amino acids and  $\alpha$ -aminoamides results in novel anticonvulsant compounds with significant effects on slow and fast inactivation of voltage-gated sodium channels and in the treatment of neuropathic pain. *ACS Chem. Neurosci.* 2, 317–332.
- (23) Wang, Y., Park, K. D., Salomé, C., Wilson, S. M., Stables, J. P., Liu, R., Khanna, R., and Kohn, H. (2010) Development and characterization of novel derivatives of the antiepileptic drug lacosamide that exhibit far greater enhancement in slow inactivation of voltage-gated sodium channels. *ACS Chem. Neurosci.* 2, 90–106.
- (24) Hodgkin, A. L., and Huxley, A. F. (1952) The dual effect of membrane potential on sodium conductance in the giant axon of *Loligo*. *J. Physiol.* 116, 497–506.
- (25) Rudy, B. (1978) Slow inactivation of the sodium conductance in squid giant axons. Pronase resistance. *J. Physiol.* 283, 1–21.
- (26) Bean, B. P. (2007) The action potential in mammalian central neurons. *Nat. Rev. Neurosci.* 8, 451–465.
- (27) Do, M. T. H., and Bean, B. P. (2003) Subthreshold sodium currents and pacemaking of subthalamic neurons: Modulation by slow inactivation. *Neuron* 39, 109–120.
- (28) Vilin, Y. Y., and Ruben, P. C. (2001) Slow inactivation in voltage-gated sodium channels: molecular substrates and contributions to channelopathies. *Cell Biochem. Biophys.* 35, 171–190.
- (29) Errington, A. C., Stöhr, T., and Lees, G. (2005) Voltage gated ion channels: Targets for anticonvulsant drugs. *Curr. Top. Med. Chem.* 5, 15–30.
- (30) Toledo-Aral, J. J., Moss, B. L., He, Z. J., Koszowski, A. G., Whisenand, T., Levinson, S. R., Wolf, J. J., Silos-Santiago, I., Haleboua, S., and Mandel, G. (1997) Identification of PN1, a predominant voltage-dependent sodium channel expressed principally in peripheral neurons. *Proc. Natl. Acad. Sci. U.S.A.* 94, 1527–1532.
- (31) Rush, A. M., Dib-Hajj, S. D., Liu, S., Cummins, T. R., Black, J. A., and Waxman, S. G. (2006) A single sodium channel mutation produces hyper- or hypoexcitability in different types of neurons. *Proc. Natl. Acad. Sci. U.S.A.* 103, 8245–8250.
- (32) King, A. M., De Ryck, M., Kaminski, R., Valade, A., Stables, J. P., and Kohn, H. (2011) Defining the structural parameters that confer anticonvulsant activity by the site-by-site modification of (R)-N'-benzyl 2-amino-3-methylbutanamide. *J. Med. Chem.* 54, 6432–6442.
- (33) Catterall, W. A., Dib-Hajj, S., Meisler, M. H., and Pietrobon, D. (2008) Inherited neuronal ion channelopathies: new windows on complex neurological diseases. *J. Neurosci.* 28, 11768–11777.
- (34) Brittain, J. M., Wang, Y., Wilson, S. M., and Khanna, R. (2012) Regulation of CREB signaling through L-type Ca(2+) channels by Nipsnap-2. *Channels (Austin)* 6, 94–102.
- (35) Ma, C., and LaMotte, R. H. (2005) Enhanced excitability of dissociated primary sensory neurons after chronic compression of the dorsal root ganglion in the rat. *Pain* 113, 106–112.